Liquid Structure, Thermodynamics, and Mixing Behavior of Saturated Hydrocarbon Polymers. 2. Pair Distribution Functions and the Regularity of Mixing

Janna K. Maranas

Department of Chemical Engineering, The Pennsylvania State University, University Park, Pennsylvania 16802

Sanat K. Kumar

Department of Materials Science and Engineering, The Pennsylvania State University, University Park, Pennsylvania 16802

Pablo G. Debenedetti and William W. Graessley*

Department of Chemical Engineering, Princeton University, Princeton, New Jersey 08544

Maurizio Mondello and Gary S. Grest

Corporate Research Laboratories, Exxon Research and Engineering Company, Annandale, New Jersey 08801

Received December 2, 1997; Revised Manuscript Received July 6, 1998

ABSTRACT: The role of liquid structure in the mixing properties of saturated hydrocarbon polymers was investigated using the intermolecular pair distribution functions obtained by molecular dynamics simulations. A correlation was noted between specific geometric features of the pure component distribution functions and various observations on macroscopic mixing characteristics relative to the solubility parameter formalism—regularity, attractive irregularity, repulsive irregularity—found earlier from neutron scattering studies of their blends. Ten component pairs are represented in these comparisons, and without exception they support the correlation. To our knowledge, it is the first relationship that provides an unambiguous connection between the pure component properties of polymers and how they mix.

Introduction

This paper and the preceding one[1] describe and discuss the results of a molecular dynamics simulation study of several model polyolefin species in the liquid state. The work had two aims, to clarify the relationship between cohesive energy density Π_{CED} and internal pressure Π_{IP} in polyolefin melts, and to gain some microscopic understanding of the interactions that govern the phase behavior of their blends. The first paper describes the simulation model and compares the resulting values of Π_{CED} and Π_{IP} for oligomers (the C30 series) of seven polyolefins—polyethylene (PE), polypropylene (PP), head-to-head polypropylene (hhPP), poly(1-butene) (PB), poly(ethylene-*alt*-propylene) (PEP), poly(ethylene-*alt*-1-butene) (PEB), and polyisobutylene (PIB). Data for three of the species—PE, PP, and hhPP—were extrapolated to the polymeric range, and the results were compared with the experimental observations derived from regular mixtures of polyolefin components. The findings were consistent in broad outline with recent studies based on the PRISM model,[2−7] namely that the interactions governing phase behavior are primarily enthalpic and that they originate from differences in the local packing of chain units.

The main concern of this paper is the microscopic origin of the mixing characteristics themselves, whether the mixing of two components is *regular*, i.e., in accord with solubility parameter formalism, *stabilized irregular*, denoting enhanced miscibility relative to the solubility parameter prediction, or *destabilized irregular*, denoting a reduced miscibility.[8] In quantitative terms,

$$X_E = X_{obs} - (\delta_2 - \delta_1)^2 \tag{1}$$

where δ_1 and δ_2 are the component solubility parameters, assigned as explained elsewhere,[8] X_{obs} is the interaction density coefficient for the blend, obtained by neutron scattering measurements, and the difference, X_E, quantifies the extra interaction density. The three categories of mixing behavior correspond to[9]

$$\begin{aligned} &\text{regular:} && |X_E| \lesssim +2.5 \times 10^{-3}\ \text{(MPa)} \\ &\text{stabilized irregular:} && X_E \lesssim -2.5 \times 10^{-3}\ \text{(MPa)} \\ &\text{destabilized irregular:} && X_E \gtrsim +2.5 \times 10^{-3}\ \text{(MPa)} \end{aligned} \tag{2}$$

where X_{obs} is typically of order 30×10^{-3} MPa or more.

Pair distribution functions[10] were generated at 150 °C for the C30 series and for other chain lengths in selected cases, as described in ref 1. Both total and intermolecular pair distributions were calculated:

$$[g(r)]_{total} = \frac{\langle \rho(\mathbf{r}')\rho(\mathbf{r}' + \mathbf{r}) \rangle}{\langle \rho(\mathbf{r}') \rangle^2} \tag{3}$$

S0024-9297(97)01756-7 CCC: $15.00
Published on Web 09/12/1998

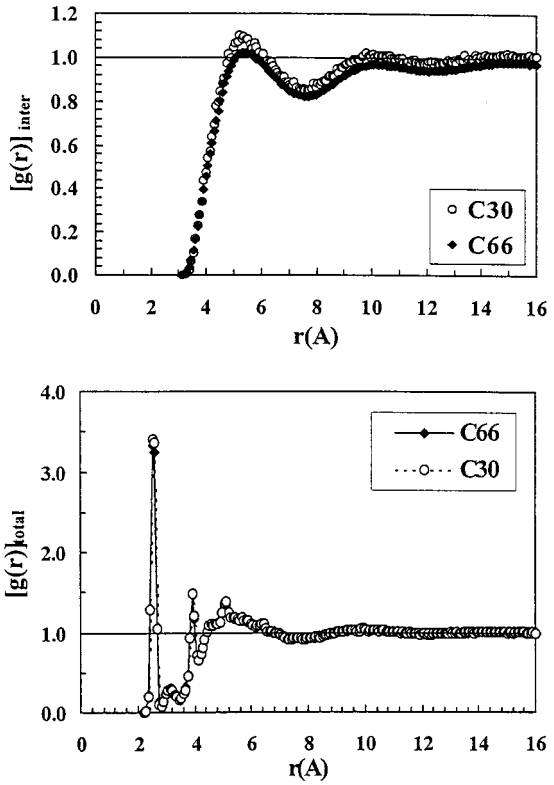

Figure 1. Total and intermolecular pair distribution functions for PE. The upper graph is $[g(r)]_{inter}$; the lower graph is $[g(r)]_{total}$.

$$[g(r)]_{inter} = \frac{\langle \rho(\mathbf{r}')[\rho(\mathbf{r}' + \mathbf{r})]_{inter} \rangle}{\langle \rho(\mathbf{r}') \rangle^2} \quad (4)$$

in which $\rho(\mathbf{r}')$ and $\rho(\mathbf{r}' + \mathbf{r})$ are the instantaneous densities of united atoms at locations r′ and $\mathbf{r}' + \mathbf{r}$, the subscripts "inter" in eq 4 mean that only pairs on different molecules are counted, and the angle brackets indicate averages of all $\mathbf{r}'$ locations of united atoms in the simulation box, with $\langle \rho(\mathbf{r}') \rangle$ equal to the macroscopic density ρ. The total pair distribution (eq 3) is obtainable from wide-angle X-ray scattering (WAXS) experiments.[11] However, it is the intermolecular part, $[g(r)]_{inter}$, that is relevant to the thermodynamics of mixing. For simulations based on several varieties of united atoms in the molecule, and with the usual central forces and pairwise additive assumptions,

$$\Pi_{CED} = -\frac{\rho^2}{2}\int_0^\infty 4\pi r^2 \sum_i \sum_j \psi_{ij}(r)[g_{ij}(r)]_{inter}\, dr \quad (5)$$

in which $\psi_{ij}(r)$ is the intermolecular potential for i,j united atom pairs, and $[g_{ij}(r)]_{inter}$ is the corresponding pair distribution for i,j pairs on different molecules. The intermolecular pair distribution could, in principle, be obtained from neutron scattering data for mixtures of the hydrogenous and deuterated versions of the same species, although those experiments apparently have not been done. It can also be obtained by subtracting $[g(r)]_{inter}$, as calculated by a theory such as PRISM,[12] from $[g(r)]_{total}$ obtained by WAXS. A few evaluations of $[g_{ij}(r)]_{inter}$ were made in the simulation study,[13] but in this paper we consider only the average, $[g_{ij}(r)]_{inter}$.

Results and Discussion

The total and intermolecular pair distributions are compared in Figures 1−3 for oligomeric polyethylene, polypropylene, and polyisobutylene. As discussed separately,[14] the simulations of $[g(r)]_{total}$ agree rather well with the WAXS results for these and other polymer species.[11] The simplicity of $[g(r)]_{inter}$ relative to $[g(r)]_{total}$ is evident. Also, while careful examination of $[g(r)]_{total}$ distinguishes the results from one polymer species to another, the differences are immediately obvious in $[g(r)]_{inter}$. Thus, $[g(r)]_{inter}$ for polyethylene has two peaks and possibly a third, indicating a significant amount of intermolecular liquid structure, while $[g(r)]_{inter}$ for polypropylene simply rises monotonically to unity, indicating little liquid structure beyond the hard-core repulsion which sets in near $r = 3.1$ Å. The behavior of polyisobutylene is intermediate: there are two peaks in $[g(r)]_{inter}$, but both are weak compared with those for polyethylene. All these results are slightly dependent on chain length, as shown in Figure 1, but the qualitative differences among species are not affected by chain length.

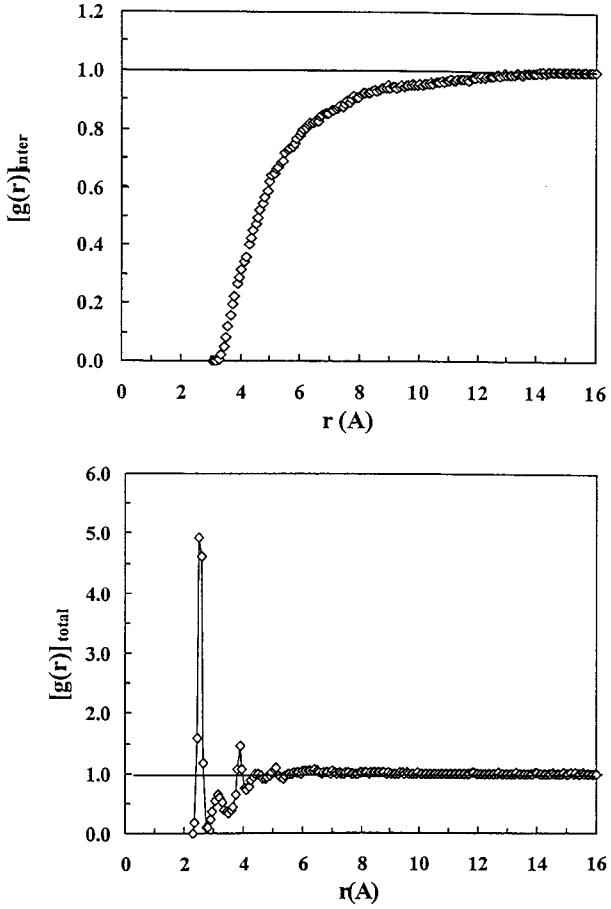

Figure 2. Total and intermolecular pair distribution functions for iPP. The upper graph is $[g(r)]_{inter}$; the lower graph is $[g(r)]_{total}$.

Differences in $[g(r)]_{inter}$ track the differences in effective aspect ratio, as defined in ref 6. Effective aspect ratio is a measure of both chain diameter and chain flexibility. Thus, PE, with no branching and a large characteristic ratio, has the largest aspect ratio of all materials considered here. The remainder, in order of increasing aspect ratio, are PEP, PIB, PP, and PB. This series corresponds to decreasing liquid structure, as reflected in $[g(r)]_{inter}$.

Intermolecular pair distributions for PE, PEP, hhPP, and PP—species with varying frequencies of methyl branching—are compared in Figure 4. Comparisons of

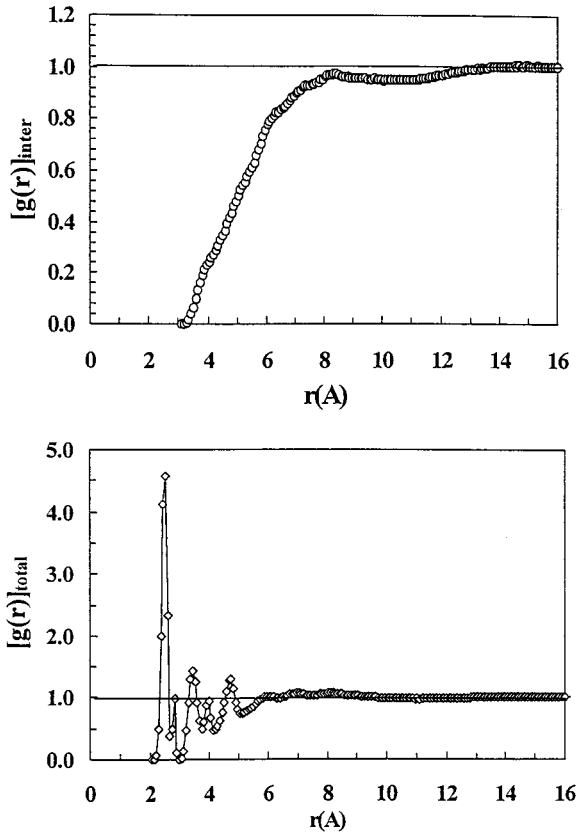

Figure 3. Total and intermolecular pair distribution functions for PIB. The upper graph is $[g(r)]_{inter}$; the lower graph is $[g(r)]_{total}$.

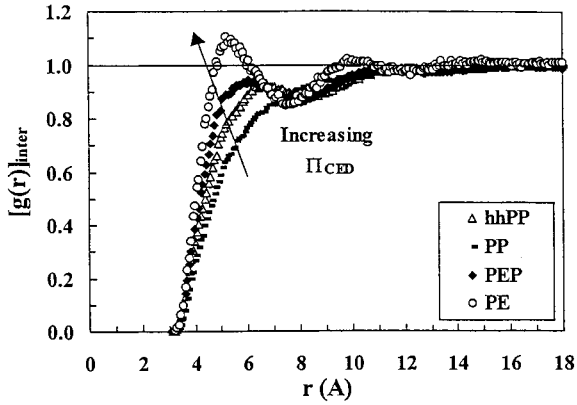

Figure 4. Intermolecular pair distributions for polyolefin species with methyl branches. The arrow indicates the direction of increasing cohesive energy density: PE > PEP > hhPP > PP.

$[g(r)]_{inter}$ for methyl and ethyl branching in species with the same branching frequency are shown in Figure 5 for PEP and PEB, and in Figure 6 for PP and PB. A variety of $[g(r)]_{inter}$ forms are evident among the seven species. Solubility parameters are available for six of the seven. The exception is PIB, whose mixtures are irregular in all blends tested to date.[15] Lacking solubility parameter data for PIB and uncertain about some aspects of its simulation model,[1] we have omitted PIB from the comparisons that follow.

Data on mixing characteristics are available for 10 blends of the six species with one another.[9] They are listed with their mixing category in Table 1. With pure component pair distributions assigned to one of three categories shown in Figures 1 (structured), 2 (unstructured), and 3 (intermediate), we find a qualitative correlation in mixing behavior among these 10 blends with the differences in shapes of the component pair distribution functions. Thus, if the shapes belong to the same category, the blend is destabilized; i.e., the single-phase state is less stable than predicted by regular mixing theory. If the shapes are quite different, the single phase is more stable than predicted. Regularity of mixing, represented here only by the PEP/PEB blend, corresponds to the crossover, an intermediate difference in the pure component $[g(r)]_{inter}$ shapes.

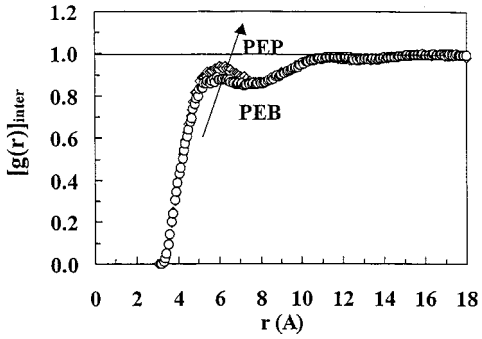

Figure 5. Intermolecular pair distributions for PEP and PEB. The chemical structures differ only in branch length (methyl, ethyl); the arrow indicates increasing cohesive energy density: PEP > PEP.

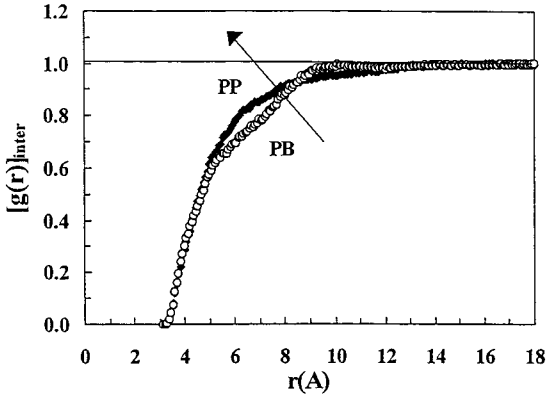

Figure 6. Intermolecular pair distributions for PP and PB. The chemical structures differ only in branch length (methyl, ethyl). The arrow indicates increasing cohesive energy density: PP > PB.

Table 1. Difference in Component Liquid Structure and Mixing Behavior

component pair	obsd mixing behavior	$[g(r)]_{inter}$ shapes
hhPP/PEP	destabilized	similar
hhPP/PEB	destabilized	similar
PP/PB	destabilized	similar
PP/PEB	(immiscible)	similar
PEP/PEB	regular	intermediate
PP/PEP	stabilized	different
PP/hhPP	stabilized	different
PP/PEB	stabilized	different
PE/PEP	stabilized	different
PE/PB	stabilized	different

In an effort to make the comparisons more quantitative, we devised a simple and admittedly crude scheme for quantifying the liquid structure, as evidenced in the shape of $[g(r)]_{inter}$. As indicated in Figure 7, the first peak position is denoted by r_p, and the difference between $[g(r)]_{inter}$ at the first peak and its value at the following minimum is denoted by d. The values of r_p and d for the various species are given in Table 2. Also

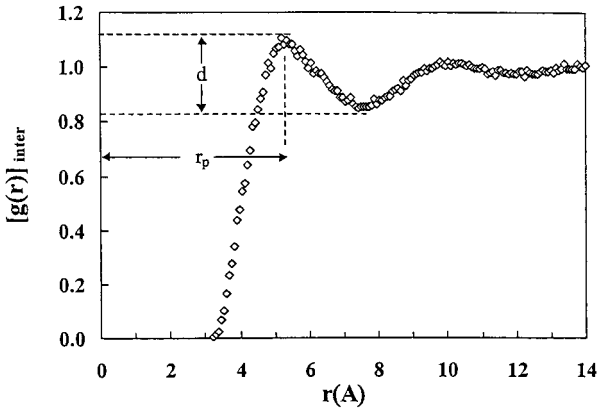

Figure 7. Liquid structure characteristics.

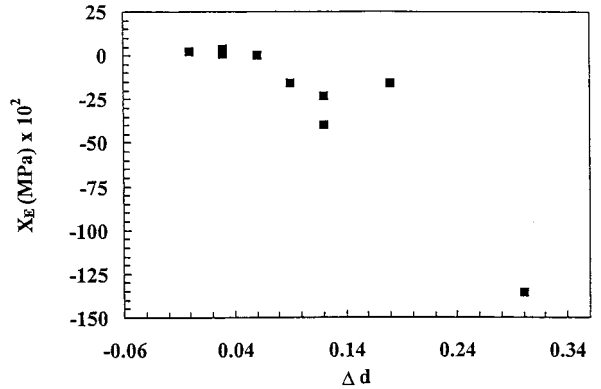

Figure 8. Correlation of excess interaction density with difference in component liquid structure.

Table 2. Branch Frequency and $[g(r)]_{inter}$ Characteristics

polymer	branches backbone carbons	r_{peak} (Å)	d
PE	0.00	5.6	0.30
PEP	0.25	6.0	0.12
PEB	0.25	6.0	0.06
PP	0.50	*a*	(0)
hhPP	0.50	6.5	0.09
PB	0.50	*a*	(0)
PIB	1.00	(8.0)[b]	(0.03)[b]

[a] No peaks in $[g(r)]_{inter}$. [b] Values for PIB are uncertain, as discussed in the text.

Table 3. Mismatch in Component Liquid Structures and Excess Interaction Density in the Mixture at 121 °C

component pair	X_E (MPa) × 10^2	$\|\Delta d\|$
PE/PB	−136	0.30
PB/PEP	−40	0.12
PP/PEP	−23	0.12
PE/PEP	−16	0.18
PP/hhPP	−16	0.09
PP/PB	−1	(0)
PEP/PEB	<|0.25|	0.06
hhPP/PEP	0.3	0.03
hhPP/PEB	3.4	0.03
PP/PEB	immiscible	0.06

listed is the average number of branches per backbone carbon, a parameter of the chemical structure that, perhaps not surprisingly, seems to correlate with r_p. Values of the extra interaction density coefficient X_E at 121 °C for the various blends[9] are listed in Table 3. Also listed is $|\Delta d|$, the magnitude of the difference in the structural parameter d for the components. From the plot of X_E as a function of $|\Delta d|$ in Figure 8, it is evident that a reasonable correlation exists between the extra interaction density in a blend and this simple measure

Table 4. Blend Component Types and Mixing Characteristics

components	regular	irregular
homopolymer/homopolymer	1	11
homopolymer/copolymer	∼20	7
copolymer/copolymer	∼100	1

of the difference in intermolecular liquid structure for the components.

The question of regular mixing has been addressed with PRISM-based studies, primarily in ref 5, where it was also found that differences in local packing had an influence on mixing behavior. In the language of that study, most blends considered here fall into the "reinforcing" category, where the shape of $[g(r)]_{inter}$ mismatch is in the same direction of the energetic mismatch, as we find that $[g(r)]_{inter}$ correlates directly with solubility parameter values for all materials considered, with the possible exception of PIB.[15] Within this reinforcement regime, we find all three types of mixing behavior, stabilizing irregular, destabilizing irregular, and regular.

The number of blends in the test is still rather too small to justify sweeping conclusions, so we put forward these suggestions in tentative fashion, hoping they might be of some use in guiding future studies. A possible explanation for these observations is offered in the following section.

Concluding Remarks

It is curious that blends of components with matching $[g(r)]_{inter}$ are mildly destabilized relative to the solubility parameter prediction and, conversely, that regular mixing would appear to require a small mismatch. Large mismatch leading to relative stabilization also seems counterintuitive. However, it is at least conceivable that local packing effects could produce such results. Ignoring stereoisomeric differences, each of the species considered here, including PEP and PEB, is a homopolymer in the sense of having essentially only one repeating structure. In the liquid state, each species has some distribution of local chain conformations, dictated mainly by the intramolecular energetics. Satisfying that distribution while also satisfying local packing (space-filling) constraints might be easier in a mixture, because mixing would provide the component chains with a broader population of local conformations to choose among. Accordingly, overlaying the cohesive energy and equation-of-state costs of forming a mixture would be the packing effect, favoring mixing, in some cases at least, by the increase in local shape choices that mixing would produce.

Packing effects of this sort could also explain the striking distinctions between homopolymers and statistical copolymers in mixing characteristics. Thus, among the nearly 150 polyolefin blends we have studied thus far,[9,16−18] we observe the breakdown in mixing behavior shown in Table 4. All but one of the 19 irregular blends involve at least one homopolymer component, and only one of the 12 homopolymer−homopolymer blends is regular. Such behavior could be interpreted as follows. A statistical copolymer by itself provides a broad range of local shapes, so relatively little enhancement in space-filling efficiency is gained upon mixing. Hence, pairs of copolymers mix in regular fashion, i.e., in accord with their differences in cohesive energy density. Homopolymer−copolymer pairs behave

in intermediate fashion, with a far larger proportion mixing regularly than homopolymer pairs, but still with a significant number that mix irregularly. Thus, although admittedly speculative, this packing idea does seem to account for a number of otherwise unexplained observations about the mixing behavior of saturated hydrocarbon polymer species.

Acknowledgment. Funding for this work was provided by the National Science Foundation through Grants CTS97-04907 and DMR98-04327 (S.K.K.) and DMR93-10762 (W.W.G.), and by the Department of Energy through Grant DE-FG02-87ER13714 (P.G.D.). We are grateful to Dr. Mark Disko of Exxon Corporate Laboratories for sharing with us some results for pair distributions obtained by full atom simulations. We are also grateful to K. S. Schweizer for numerous helpful comments and criticisms.

References and Notes

(1) Maranas, J. K.; Mondello, M.; Grest, G. S.; Kumar, S.; Debenedetti, P. G.; Graessley, W. W. *Macromolecules* 1998, *31*, 6991.
(2) Weinhold, J. D.; Kumar, S. K.; Singh, C.; Schweizer, K. S. *J. Chem. Phys.* **1995**, *103*, 9460.
(3) Singh, C.; Schweizer, K. S. *J. Chem. Phys.* **1995**, *103*, 5418.
(4) Schweizer, K. S. *Macromolecules* **1993**, *26*, 6050.
(5) Singh, C.; Schweizer, K. S. *Macromolecules* **1995**, *28*, 8692; **1997**, *30*, 1490.
(6) Schweizer, K. S.; Singh, C. *Macromolecules* **1995**, *28*, 2063.
(7) Schweizer, K. S.; David, E. F.; Singh, C.; Curro, J. G.; Rajasekaran, J. J. *Macromolecules* **1995**, *28*, 1528.
(8) Krishnamoorti, R.; Graessley, W. W.; Balsara, N. P.; Lohse, D. J. *Macromolecules* **1994**, *27*, 3073. (b) Graessley, W. W.; Krishnamoorti, R.; Reichart, G. C.; Balsara, N. P.; Fetters, L. J.; Lohse, D. J. *Macromolecules* **1995**, *28*, 1260.
(9) Krishnamoorti, R.; Graessley, W. W.; Dee, G. T.; Walsh, D. J.; Fetters, L. J.; Lohse, D. J. *Macromolecules* **1996**, *29*, 367.
(10) Hansen, J. P.; McDonald, I. R. *The Theory of Single Liquids*, 2nd ed.; Academic Press: Orlando, FL, 1986.
(11) Londono, J. D.; Habenschuss, A.; Curro, J. G.; Rajasekaran, J. J. *J. Polym. Sci.: Part B, Polym. Phys.* **1996**, *34*, 3055.
(12) Rajasekaran, J. J.; Curro, J. G., *J. Chem. Soc., Faraday Trans.* **1995**, *91*, 2427.
(13) Maranas, J. K. Ph.D. Thesis, Princeton University, 1997.
(14) Londono, J. D.; Maranas, J. K.; Mondello, M.; Habenschuss, A.; Grest, G. S.; Graessley, W. W.; Debenedetti, P. G.; Kumar, S. K. *J. Polym. Sci.: Polym. Phys.*, in press.
(15) Krishnamoorti, R.; Graessley, W. W.; Fetters, L. J.; Garner, R. T.; Lohse, D. J. *Macromolecules* **1995**, *28*, 1252.
(16) Reichart, G. C.; Graessley, W. W.; Register, R. A.; Krishnamoorti, R.; Lohse, D. J. *Macromolecules* **1997**, *30*, 3036.
(17) Reichart, G. C.; Graessley, W. W.; Register, R. A.; Krishnamoorti, R.; Lohse, D. J. *Macromolecules* **1997**, *30*, 3363.
(18) Reichart, G. C.; Graessley, W. W.; Register, R. A.; Lohse, D. J. *Macromolecules*, in press.

MA971756U